RL 259
Rev. 7/29/64

THE BACK SCATTERING CROSS SECTION OF A CONE-SPHERE

by

T. B. A. Senior*

SUMMARY

The metallic cone-sphere is the prototype for many low cross section shapes and has received an increasing amount of attention in recent years. In spite of the simplicity of its mathematical form, it is still one for which no exact solution of the boundary-value problem is available, and to calculate the cross section we must rely on approximate methods with such refinements and extensions as experimental data demands. We here present some new data for both the back scattered and surface fields at nose-on incidence and deduce therefrom a modification to the accepted theory sufficient to explain the results.

---

* The research reported in this paper was supported by the Air Force Cambridge Research Laboratories under Contract AF 19(604)-6655.

** Radiation Laboratory, The University of Michigan, Ann Arbor, Michigan.

INTRODUCTION

The design of shapes to have a low back scattering cross section for some range of aspect angles is a problem of continued interest in scattering theory. To remove the possibility of any specular reflection at these aspects, the chosen shape is often a pointed body of revolution, smoothly terminated at the rear to minimize the contribution from any ring singularity there, and a typical example of this configuration is the cone-sphere (or 'carrot') in which the first derivatives of the surface profile are matched at the join. Although it has not been demonstrated that this is in any sense an optimum as regards its cross sectional behavior at nose-on aspects, it does at least have the advantage of a relatively simple mathematical form, but even so it is still a shape for which no exact solution of the boundary-value problem is available. In consequence, to calculate the scattering cross section it is necessary to rely on approximate methods such as physical optics, creeping wave theory, etc., with the accuracy of the predictions judged by comparison with experimental data.

The first reported measurement of a cone-sphere was by Sletten[1] who employed this shape to simulate a semi-infinite cone, but it was not until 1960 that a reasonably complete set of data was published. Using a Doppler system operating at a wavelength of 3.22 cm, Gent et al[2] measured the nose-on cross section of 50 cone-spheres with vertex angle 30° and base radii a spanning the range $1.00 \leqslant a/\lambda \leqslant 2.125$, and from an analysis of the results the magnitudes of the contributing components were deduced. Additional data for cone-spheres of the same angle was later obtained by Kennaugh and Moffatt[3] and Moffatt[4] who measured six models of different sizes with a variable frequency X-band system to give 39 cross section values in the range $1 \leqslant ka < 7$, where $k = 2\pi/\lambda$. When these were compared with the predictions of physical optics, the geometrical theory of diffraction[5] and the 'impulse approximation' method[6], the superiority of this last approach was clearly apparent, but a systematic discrepancy between theory and experiment still remained. This was pointed out by Blore[7], who measured cone-spheres of angles 15, 30, 40, 60 and 75° to produce the most comprehensive body of data yet available for his shape. For each cone angle the cross section was determined for as many as 100 values of ka ranging from (about) 0.3 up to 7.5 using five large sets of models and a combination of X and K_a-band frequencies. At the lower end of the interval the results are in good agreement with the modified Rayleigh formula proposed by Siegel[8], and this in turn matches in remarkably well with the impulse approximation curve. For ka greater than (about) 2, however, the curve lies two or more db below the measured peak values of the cross section and as much as 7db below the minima, with some evidence of a displacement in the position of the latter. Though the overall agreement is, nevertheless, quite gratifying, an understanding of the nature of the discrepancy is important for its own sake as well as for the effect that it may have on estimates of the scattering cross sections of other and more general shapes, and a study was therefore undertaken to discover its origin. It is the purpose of this paper to detail the investigation.

2. Basic Theory

It is appropriate to begin with a review of the basic theory as it applies to the calculation of the nose-on cross section for values of the base radius greater than a wavelength or so.

Consider a perfectly conducting cone-sphere of semi-vertex angle α and base radius a illuminated by a plane wave at nose-on incidence. In terms of a Cartesian coordinate system (x, y, z) whose origin is at the center of the spherical cap, the axis of the cone is taken as the z axis, and since there is no loss of generality in choosing the electric vector to lie in the x direction, we write

$$\underline{E}^i = \hat{x} e^{-ikz}$$

where a time factor $e^{-i\omega t}$ has been assumed and suppressed. From symmetry the back scattered field has the same polarization as the incident field and hence, in the far zone, we can define a scattering amplitude S by the equation

$$\underline{E}^s = \hat{x} \frac{e^{ikr}}{kr} S$$

from which it follows that

$$\sigma = \frac{\lambda^2}{\pi} \left| S \right|^2 . \tag{1}$$

If the physical optics approximation is applied, the determination of the scattered field is reduced to quadratures, and the resulting expression for S is[9]

$$S = -\frac{i}{4} \left(\tan^2\alpha \, e^{-2ika \operatorname{cosec} \alpha} - \sec^2\alpha \, e^{-2ika \sin \alpha} + 1 \right) . \tag{2}$$

The sources of the individual terms can be identified by the phase factors. Thus, the first term is associated with the tip, the second with the cone-sphere join and the third with the shadow boundary. The cross section attributable to the tip is therefore

$$\sigma_{tip} = \frac{\lambda^2}{16\pi} \tan^4 \alpha \tag{3}$$

and this is in general agreement with the result obtained from the exact solution for scattering by a semi-infinite cone[9]. The cross section of the join is similarly

$$\sigma_{join} = \frac{\lambda^2}{16\pi} \sec^4 \alpha, \tag{4}$$

which has the same wavelength dependence as the tip contribution, but a much greater magnitude. Thus, for example, when $\alpha = 15^0$

$$\sigma_{tip} = 1.026 \times 10^{-4} \lambda^2$$

whereas

$$\sigma_{join} = 2.286 \times 10^{-2} \lambda^2,$$

and though there is as yet no exact analysis to support the formula, it is believed to give a valid estimate of the return from the join when the first derivatives of the surface profile are matched. Since the surface in the neighborhood of the join is entirely in the illuminated region, the current distribution on which (4) is based should not be seriously in error for $ka \cos \alpha >> 1$.

For the shadow boundary contribution the physical optics answer is spurious and arises because of the current discontinuity introduced by this approximation independently of the presence of the cone. From an analysis of the field scattered by a sphere it is found that the return from the boundary is produced by creeping waves, which are launched in the vicinity of this point and arrive at the receiver only after having traversed the rear of the body. Since the separation (in wavelengths) between the cone-sphere join and the shadow boundary increases with increasing frequency, it seems reasonable that this contribution should be determinable by reference to the sphere alone, and in place of the third term in equation (2) we now have[10]

$$S_c = \left(\frac{ka}{2}\right)^{4/3} e^{i\pi(ka-2/3)} \frac{1}{\{\beta\, Ai(-\beta)\}^2} \left\{ 1 + \frac{8\beta}{15}\left(1+\frac{9}{32\beta}\right)\left(\frac{2}{ka}\right)^{2/3} e^{i\frac{\pi}{3}} \right\}$$
$$\cdot \exp\left\{ -\beta\pi\left(\frac{ka}{2}\right)^{1/3} e^{-i\frac{\pi}{6}} - \frac{\beta^2\pi}{60}\left(1-\frac{9}{\beta^3}\right)\left(\frac{2}{ka}\right)^{1/3} e^{i\frac{\pi}{6}} \right\} \qquad (5)$$

where

$$\beta = 1.01879\ldots \quad \text{and} \quad Ai(-\beta) = 0.53565\ldots$$

This is a more complete expression for the major creeping wave component than is usually employed, and is accurate to about one percent for ka $\geqslant$ 5. At still lower frequencies, however, even (5) becomes inadequate owing to the increased importance of the higher order waves, and no simple formula is then available. Nevertheless, numerical values can be obtained by subtracting the specular return for a sphere (Logan[11]) from the complete scattering amplitude computed from the Mie series. This has been done by Gent et al[2] for selected values of ka and, implicitly, by Kennaugh and Moffatt[6].

If this new prescription for cone-sphere scattering is basically correct, certain conclusions follow immediately. Since the creeping wave is exponentially attenuated with increasing ka, it contributes nothing to the high frequency limit, and hence

$$S = -\frac{i}{4}\left\{\tan^2\alpha\, e^{-2ika\,\mathrm{cosec}\,\alpha} - \sec^2\alpha\, e^{-2ika\sin\alpha}\right\}$$

for sufficiently large ka. The first term is also negligible in comparison with the second, so that finally

$$S \sim \frac{i}{4}\sec^2\alpha\, e^{-2ika\sin\alpha} \tag{6}$$

and this is reasonably consistent with data for the largest ka at which measurements have been made.

In most cases, however, the intermediate values of ka are of more practical interest. The creeping wave now gives a significant contribution and if we again neglect the tip return, the scattering amplitude can be written as

$$S = \frac{i}{4}\sec^2\alpha\, e^{-2ika\sin\alpha} + S_c\,. \tag{7}$$

The cross section which then results is identical to that obtained by Kennaugh and Moffatt[3] using the impulse approximation technique, but differs from the formula originally proposed by Keller[5] through the inclusion of a return from the cone-sphere join, the neglect of the tip contribution, and the use of a more complete expression for the creeping wave component.

3. Experiment

From a consideration of equation (5) it is seen that the phase difference between the two terms on the right hand side of (7) is essentially a linear function of ka for $ka \gg 1$, and by comparison the amplitude of S_c is slowly varying. The nose-on cross section will therefore oscillate as a function of ka in a manner which is almost sinusoidal in any small interval, and in practice the oscillations are significant from the edge of the Rayleigh region up to $ka = 100$ or more. Under these circumstances it is obvious that for a valid check on equation (7) the cross section should be measured at a series of closely spaced values of ka sufficient to embrace one or more periods of the oscillations, and by comparison isolated determinations are of relatively little worth.

To get such data, either a or λ (or both) must be varied. The first method automatically implies a large group of models each slightly different in size from the others, and this is the technique by which most of the more comprehensive sets of data have been obtained so far. There is, however, a disadvantage associated with it. If the cone and sphere portions of the model are incorrectly mated, the scattering from the join may be profoundly disturbed. Thus, for example, a ridge at this point equivalent to an angular difference δ between the tangents to the cone and the sphere would increase the first term of (7) by a factor ϕ

$$1 + 2ika \cos \alpha \tan \delta \tag{8}$$

approximately, as follows by a straightforward application of physical optics, and the second term of (8) may easily dominate through its ka factor. The neighborhood of the join is certainly one of the most critical regions for a cone-sphere, and care is necessary to ensure accurate modeling here. Not unnaturally, the probability of imperfections increases with the number of models employed, and many of the irregularities apparent in the data of Gent et al[2] may be due to such imperfections amongst their 50 models.

The difficulty can be overcome, at least in part, by using one carefully constructed model and achieving the variation in ka by shifting frequencies, and this is the procedure that we adopted. The first model had $\alpha = 12\frac{1}{2}^{\circ}$ and a = 4.519 cm, and was made from rolled aluminum stock machined to a high degree of surface finish. For convenience, attention was directed at X-band frequencies and within the range 7.98 to 10.97 Gc a total of 17 individual frequencies were employed. All were generated from a stabilized oscillator of continuously varying frequency or from phase-locked oscillators. At each one a pattern was recorded showing the back scattered return out to the specular flash or beyond, followed by a minimum of 10 (and on average 25) separate measurements of the nose-on cross section σ / λ^2. Every effort was made to get the highest possible accuracy and to have the measurements truly independent. The means and standard deviations were then calculated, and on the assumption that the errors are random, the means should be accurate to about 0.3 db. The data is plotted as a function of ka in Fig. 1. Similar results have also been obtained for a cone-sphere of semi vertex angle $7\frac{1}{2}^{\circ}$ and base radius 5.613 cm.

The expected sinusoidal oscillation is clearly in evidence, but to determine the full extent of the agreement between the theoretical values and the measured data, it is necessary to compute S using equation (7). This in turn requires the calculation of S_c from equation (5), and for the required range of ka it is found that S_c can be written as

$$S_c = (0.5026 - 0.01467\,ka)\exp\left\{i\pi(1.0256\,ka - 0.95410)\right\}. \tag{9}$$

Note that this is purely a numerical representation based on the values computed from (5), and though accurate over the above range, it has no physical significance per se. Nevertheless, it is convenient inasmuch as it allows us to derive an explicit theoretical expression for σ/λ^2 and from equations (1), (7) and (9) with $\alpha = 12\frac{1}{2}^{\circ}$ we have

$$\frac{\sigma}{\lambda^2} = 0.02190\left|(1.916 - 0.05593\,ka) + \exp\left\{i\pi(1.45410 - 1.16335\,ka)\right\}\right|^2 \tag{10}$$

The corresponding curve is shown dashed in Fig. 1.

The predicted locations of the appropriate maxima and minimum are ka = 8.127, 9.846 and ka = 8.986. These are in excellent agreement with the data and certainly there is no indication of the displacement reported by Blore[7]. There is, however, a notable amplitude discrepancy, and the theoretical curve lies almost uniformly below the measured points. Since the maxima and minima are both too low, it would appear that the larger of the two terms in (7) should be increased, implying[12] an enhancement of the creeping wave contribution, and to see whether this alone would be sufficient, an expression of the form

$$\frac{\sigma}{\lambda^2} = 0.02190\left|A(1.916-0.05593\,ka)+B\exp\left\{i\pi(1.45410-1.16335\,ka)\right\}\right|^2 \qquad (11)$$

was postulated. The factors A and B apply to the first and second terms respectively in (7), and when (11) was fitted to the data using the method of least squares, the best fit was obtained with $A = 1.3$ and $B = 0.9$. Such a modification to (10) is sufficient to reproduce even the small decrease in the amplitudes of the successive measured maxima, and the closeness of the fit strongly suggests that there is some mechanism operating whereby the amplitude of the creeping wave is increased over and above the value that it would have for a sphere of the same size. An increase of between 2 and 3db would remove most of the discrepancy evident in Fig. 1, and by comparison the slight reduction in the join contribution produced by the least squares analysis is not felt to be significant. The value of B is strongly influenced by the measured data near to the minimum in the cross section curve, and this is where the experimental points are most likely to be in error.

4. Creeping Wave Enhancement

An increase in the far field contribution of a creeping wave almost necessarily implies an enhancement of its value on the surface, and since the measured creeping wave amplitude on the surface of a sphere is in excellent agreement with the theoretical expression, it follows that the addition of a conical nose must in some way increase the excitation of the wave.

In an attempt to explain this phenomenon, two possible mechanisms have been investigated. The first of these is associated with the cone-sphere join alone and is independent of the rest of the cone except insofar as it would not exist were the cone not there. At the join the first derivative of the surface profile is continuous, but it still constitutes a singularity (albeit a weak one) by virtue of the discontinuity in the second and higher derivatives. It is therefore possible that it could increase the field intensity in the vicinity of the shadow boundary either through its radiated field or, equivalently, by the excitation of a creeping wave which is in phase with that generated by the sphere itself. Although there is no canonical problem whose solution is known and bears on the matter, it would appear that the situation can be modeled by a sphere with a semi-active ring slot at a position corresponding to the cone-sphere join. In the slot either or both of the tangential components of the electric field are specified as constant multiples of the incident field values, with the constant factors determined by comparison of the radiated field of the slot with the back scattered field of the cone-sphere join. A consideration of the surface field within the shadow then leads to an estimate of the extent to which the creeping waves are increased by the presence of the singularity. The increase, however, is far below the level deduced from the far field data for the cone-sphere, and it must therefore be concluded that the join is not primarily responsible for the observed enhancement.

From the failure of this first mechanism it would appear that the cone sides are not a negligible factor in the creeping wave enhancement, but to discover the precise role that they do play it is necessary to examine the currents on the surface of a sphere. These can be obtained directly from the standard Mie solution, and in terms of spherical polar angles θ and ϕ, the components of the current vector $\underline{J}$ are

$$J_\theta = -Y \cos\phi \, T_2(\theta) \tag{12}$$

$$J_\phi = Y \sin\phi \, T_1(\theta) \tag{13}$$

where Y is the intrinsic admittance of free space and[13]

$$T_1(\theta) = \frac{1}{ka} \sum_{n=1} (-i)^{n+1} \frac{2n+1}{n(n+1)} \left\{ \frac{1}{\zeta_n'(ka)} \frac{P_n^1(\cos\theta)}{\sin\theta} - \frac{i}{\zeta_n(ka)} \frac{\partial}{\partial\theta} P_n^1(\cos\theta) \right\} \tag{14}$$

$$T_2(\theta) = \frac{1}{ka} \sum_{n=1} (-i)^{n+1} \frac{2n+1}{n(n+1)} \left\{ \frac{1}{\zeta_n'(ka)} \frac{\partial}{\partial\theta} P_n^1(\cos\theta) - \frac{i}{\zeta_n(ka)} \frac{P_n^1(\cos\theta)}{\sin\theta} \right\} \tag{15}$$

where

$$\zeta_n(ka) = ka\, h_n^{(1)}(ka)$$

and the primes denote differentiation with respect to ka.

On the shadowed portion ($\theta > \pi/2$) of the sphere, $T_1(\theta)$ and $T_2(\theta)$ can be represented as sums of creeping waves, with $T_1(\theta)$ consisting mainly of 'H waves' whose magnetic vector is normal to the surface and $T_2(\theta)$ composed similarly of 'E waves.' Since the latter attenuate less then the H waves, $T_2(\theta)$ is the major current component throughout most of the shadow region. On the illuminated side, however, an optics contribution is present, and this is dominant at points well forward of the shadow boundary. Thus[14], for $ka \cos^3 \theta >> 1$

$$T_1(\theta) = -2 \cos\theta \, e^{-ika \cos\theta} \left\{ 1 + \frac{i \sin^2\theta}{2 ka \cos^3\theta} + \ldots \right\} \tag{16}$$

$$T_2(\theta) = -2 \, e^{-ika \cos\theta} \left\{ 1 - \frac{i \sin^2\theta}{2 ka \cos^3\theta} + \ldots \right\} \tag{17}$$

and by comparison any residual creeping wave effects are negligible. Note that the first term in each of (16) and (17) is identical to the physical optics prediction.

In the region intermediate to that for which (16) and (17) are appropriate and the shadow boundary, no simple expressions for $T_1(\theta)$ and $T_2(\theta)$ are available, and these must now be calculated using either the series expansions shown in (14) and (15) or the integral representations derived by Logan[15]. From such calculations it is found that for ka greater than (about) 3, $|T_1|$ and $|T_2|$ decrease more or less uniformly as θ increases from zero to $\pi/2$. The rate for T_1 is more rapid than for T_2, but even with the latter the quantity

$$\gamma' = \left| \frac{T_2(0)}{T_2\left(\frac{\pi}{2} - \alpha\right)} \right| \tag{18}$$

is appreciably greater than unity for α small and $ka > 3$ (approx.) but less than some large number dependent on α. To illustrate this behavior, $|T_2(0)|$ and $|T_2(77\frac{1}{2}^\circ)|$ have been computed for $0 \leqslant ka \leqslant 11$ using equation (15), and the results are shown in Fig. 2. As ka increases from zero, $|T_2(0)|$ increases from 1.5 to a maximum value 2.42 at $ka = 0.94$, and subsequently oscillates with a rapidly decreasing amplitude about the value 2 indicated by equation (17). It is within two percent of this value for all $ka > 4.3$. $|T_2(77\frac{1}{2}^\circ)|$ also starts with the value 1.5 at $ka = 0$, but increases more slowly to a maximum of 2.02 at $ka = 1.6$, and thereafter oscillates about a lower level which is almost constant out to the largest ka computed.. Ultimately, $|T_2(77\frac{1}{2}^\circ)|$ tends to the same limit as $|T_2(0)|$; its approach, however, is extremely slow, and even when $ka = 100$ it still differs from 2 by approximately 10 percent. For most cone-sphere applications, therefore, the values of γ' are sufficiently different from unity to be practically significant, in spite of the fact that $\gamma' \longrightarrow 1$ as $ka \longrightarrow \infty$ for all $\alpha > 0$.

Let us now consider the surface field on the conical portion of the cone-sphere. It would be convenient were we able to estimate this using the rigorous solution for (vector) scattering by a semi-infinite cone, but the complication of the exact expression is such that numerical values are not yet available. It is therefore necessary to resort to approximate methods of which physical optics is most appropriate, and from this we have for the component of current in the direction of the generators

$$J = 2Y \cos \phi \; e^{-ikz}$$

This is basically a travelling wave. Its phase is precisely that of the incident field, and consequently the wave reaches the join with a phase which is almost the same as the sphere current would have had if the sphere had been complete. Since the join is inefficient as a means of launching waves, it seems reasonable to suppose that it will also reflect little of the travelling wave energy and, finding a good match, the wave then flows over the join. Hence, just on the sphere side

$$J_\theta \simeq Y \cos \phi \, 2 e^{-ika \sin \alpha},$$

equivalent to an amplification of the original sphere current by a factor

$$\gamma = \left| \frac{2}{T_2\left(\frac{\pi}{2} - \alpha\right)} \right| . \tag{19}$$

Beyond $\theta = \frac{\pi}{2} - \alpha$, of course, the current decreases at a rate typical of the sphere alone, but the amplification through the factor γ leads to a corresponding increase in the creeping wave contributions to both the surface and far fields.

With this modification to the theory the expression for the scattering amplitude of the cone-sphere becomes

$$S = \frac{i}{4} \sec^2 \alpha \, e^{-2ika \sin \alpha} + \gamma S_c \tag{20}$$

(cf equation 7), and to show how the scattering cross section is affected, we shall again consider the example of a 25° cone-sphere.

Numerical values for γ can be obtained from equation (19) either by direct computation of $T_2\left(\frac{\pi}{2} - \alpha\right)$ using (15) or by representation of $T_2\left(\frac{\pi}{2} - \alpha\right)$ in terms of the functions

$$g^n(x) = \frac{i^n}{\sqrt{\pi}} \int_{-\infty}^{\infty} t^n e^{i\zeta t} \frac{dt}{w'(t)} \tag{21}$$

tabulated by Logan[15]. In the present case the first approach is more convenient and since $\gamma \simeq \gamma'$ for ka > 5·5, we have from Fig. 2

$$\gamma \simeq 1.189$$

for $7.5 \leqslant ka \leqslant 10.5$, based on a straight line fit to the values plotted there. The new formula for the cross section is therefore

$$\frac{\sigma}{\lambda^2} = 0.02190 \left| (2.278 - 0.06649\, ka) + \exp\left\{ i\pi\, (1.45410 - 1.16335\, ka) \right\} \right|^2 \tag{22}$$

(cf equation 10) and the corresponding curve is shown in Fig. 1. The raising of the theoretical curve has certainly removed much of the disagreement with the data, but even this enhancement of the creeping wave is not sufficient to remove all of the discrepancy.

5. Discussion

The creeping wave enhancement is a direct consequence of the difference between the true and optics values of the sphere current J_θ at the position of the join, and it may therefore seem illogical to apply the physical optics approximation to the cone and not to the sphere. Unfortunately, there is no definite criterion to indicate when physical optics can be used with confidence, and many cases are known in which the approximation gives good results even for small values of the radius of curvature. Nevertheless, the typical requirement is that all radii be large in comparison with the wavelength. Since the radius of curvature of the cone is infinite in the direction of the current flow, the expectation was that the accuracy of the approximation would be greater for the cone than the sphere, in spite of the smaller transverse radius of the former, but to verify this belief it is necessary to measure the surface field directly.

A number of such measurements have been carried out using a probe technique, and a description of the experimental equipment has been given by Senior[16]. For convenience and accuracy of operation, the frequencies have been confined to the L and S-band ranges, and even the highest S-band frequency then requires a model of larger physical size to achieve a ka value comparable to those in the far field experiment. Of the models which were available, the only one for which ka was in the range 7.5 to 10.5 was a 30° cone-sphere with base radius 10.094cm, and in Fig. 3 the measured amplitudes of the longitudinal current in the plane of the incident electric vector are presented for this case. The horizontal scale is the distance along the surface (in cm) measured from the center of the back of the sphere. The tip of the cone is to the right, and the locations of the cone-sphere join and the shadow boundary are indicated. Calibration was with respect to the incident field intensity in the plane of the support pedestal, and the frequency was 3.714 Gc corresponding to ka = 7.905. Data similar to the above, but for a frequency 3.066Gc, is given in Senior[16].

Starting at the tip the current amplitude increases rapidly over a distance of $\lambda/2$ or so, and then more slowly for a further 1.5 wavelengths.

The slight oscillation visible there may be due to a small backward-travelling wave, but this damps out in the first 2λ, by which time the amplitude is within 0.2 db of the value predicted by physical optics. It remains relatively constant up to the cone-sphere join with no evidence of any reflection from this point. Immediately beyond, however, the amplitude decreases rapidly following the trend expected of a sphere current, and to confirm this fact the cone-sphere was replaced by a sphere of the same size as the cap, and the measurements repeated for this shape. The results are also shown in Fig. 3, and though the incident field strength was again determined, <u>the relative</u> values of the currents on the two bodies are independent of the calibration. At the front of the sphere the measured amplitude is almost precisely the physical optics value, but in a distance of no more than $\lambda/2$ the amplitude has begun to fall and decreases steadily thereafter. At the position corresponding to the join it is 2.2 db below the value found with the cone-sphere, and averages some 2 db below throughout the shadow region. For the sphere itself the measured values in the illuminated region decrease somewhat more rapidly than the values computed from equation (15), and most of this is believed due to a lack of uniformity[16] in the incident field illumination. In the shadow the agreement with theory is excellent.

Based on the differences between the measured sphere and cone-sphere currents at the join, the shadow boundary and the back of the sphere, the creeping wave enhancement is found to be 2.3 db, compared with the 1.3 db obtained from equation (19). Even when an allowance is made for the irregularity of the illuminating field, the discrepancy is still greater than any intrinsic error in the measurements, and suggests an increase in the creeping wave amplitude over and above that provided by the theoretical expression for γ. Additional surface field measurements are necessary to confirm this effect, but in the meantime we note that an increase in γ of 1 db is almost precisely that required to achieve complete agreement between the predicted and measured scattering data for a 25^{o} cone-sphere (see Fig. 1).

On the other hand, it is not obvious in what way the theory should now be refined. The surface field data supports the physical optics approximation to the current on the portions of the cone sides near the join, and this in turn gives added confidence in the theoretical expression for the join contribution shown in (4). The data also confirms the existence of a creeping wave enhancement, and leaves little doubt that the theoretical picture of a travelling wave flowing over the join is basically correct. Indeed, the theoretical values of γ obtained from equation (19) have been used to predict the nose-on cross section of a 30^{o} cone-sphere for the full range of ka covered by the experimental data of Kennaugh and Moffatt[3], and to within the accuracy that the measured values can be read from their graph, the agreement with theory is almost perfect. In this respect, the cone-sphere seems akin to a flat-backed cone in that an essentially high-frequency approach is adequate for the calculation of the nose-on cross section down to the edge of the Rayleigh region. The fact that γ is an oscillatory function of ka then offers an explanation for the markedly different maximum-to-minimum ratios of the measured cross sections (Blore[7]) as the cone angle α is varied.

Acknowledgement

The author is indebted to Messrs E. F. Knott and V. V. Liepa for the measured data on the scattered and surface fields respectively.

Legends of Figures

Fig. 1. Nose-on backscattering cross section of a 25^{o} cone-sphere with base radius 4.519 cm. The numerals indicate the number of measured values whose means and standard deviations are shown. Original theory---(equation 7); modified theory —(equation 22).

Fig. 2. $T_2(0)$ and $T_2(77\frac{1}{2}^{o})$ computed from equation (17).

Fig. 3. Measured current amplitudes for a 30^{o} cone-sphere (○) and corresponding sphere (●) at 3.714 Gc.

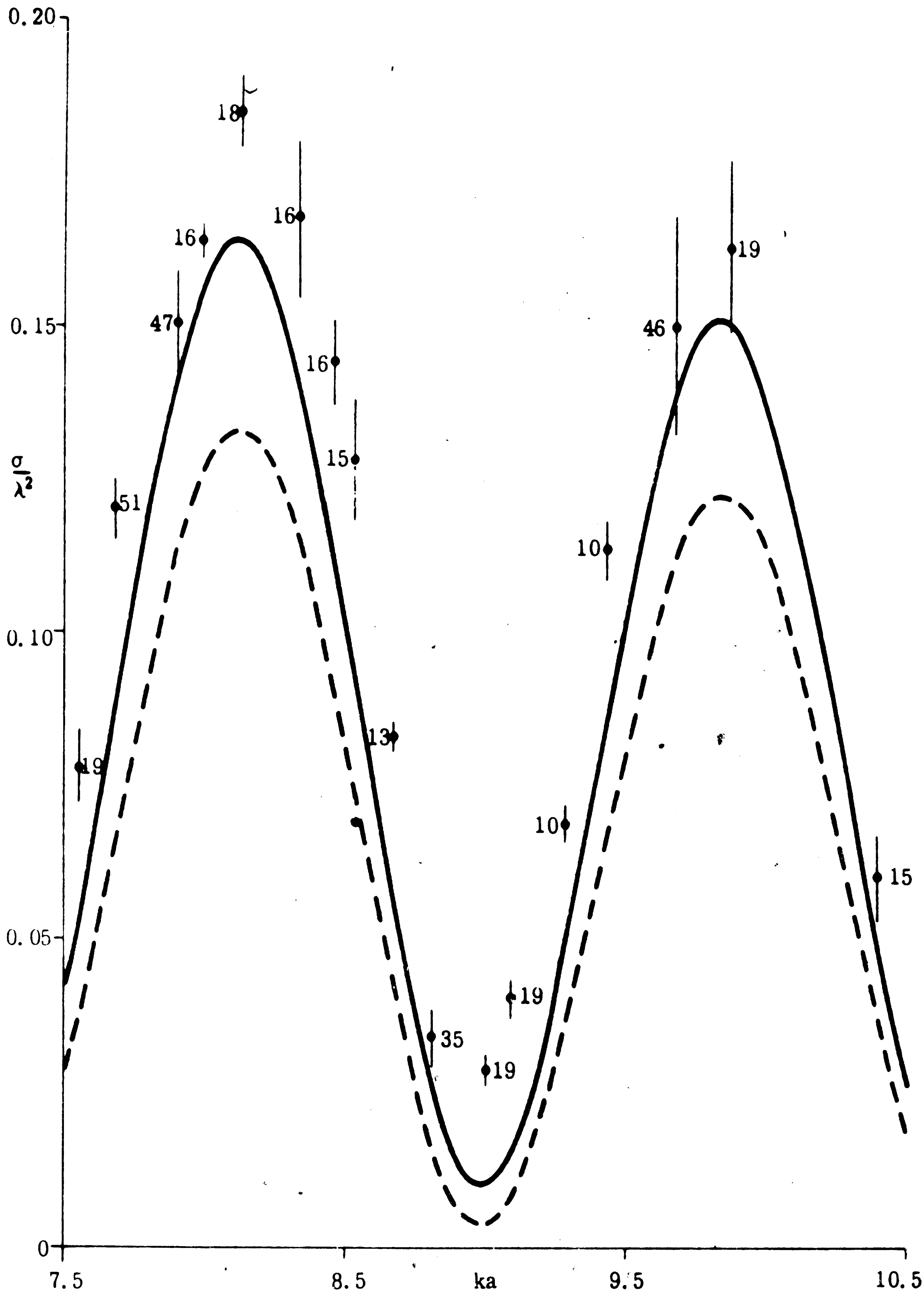

FIG. 1: Nose-on R... ...ttering Cross Section of a 25° Cone-Sphere with Base Radius 4.519cm. The numerals indicate the number of measured values whose means and standard deviations are shown. Original theory – – (Eq. 7); Modifed theory —— (eq. 20)

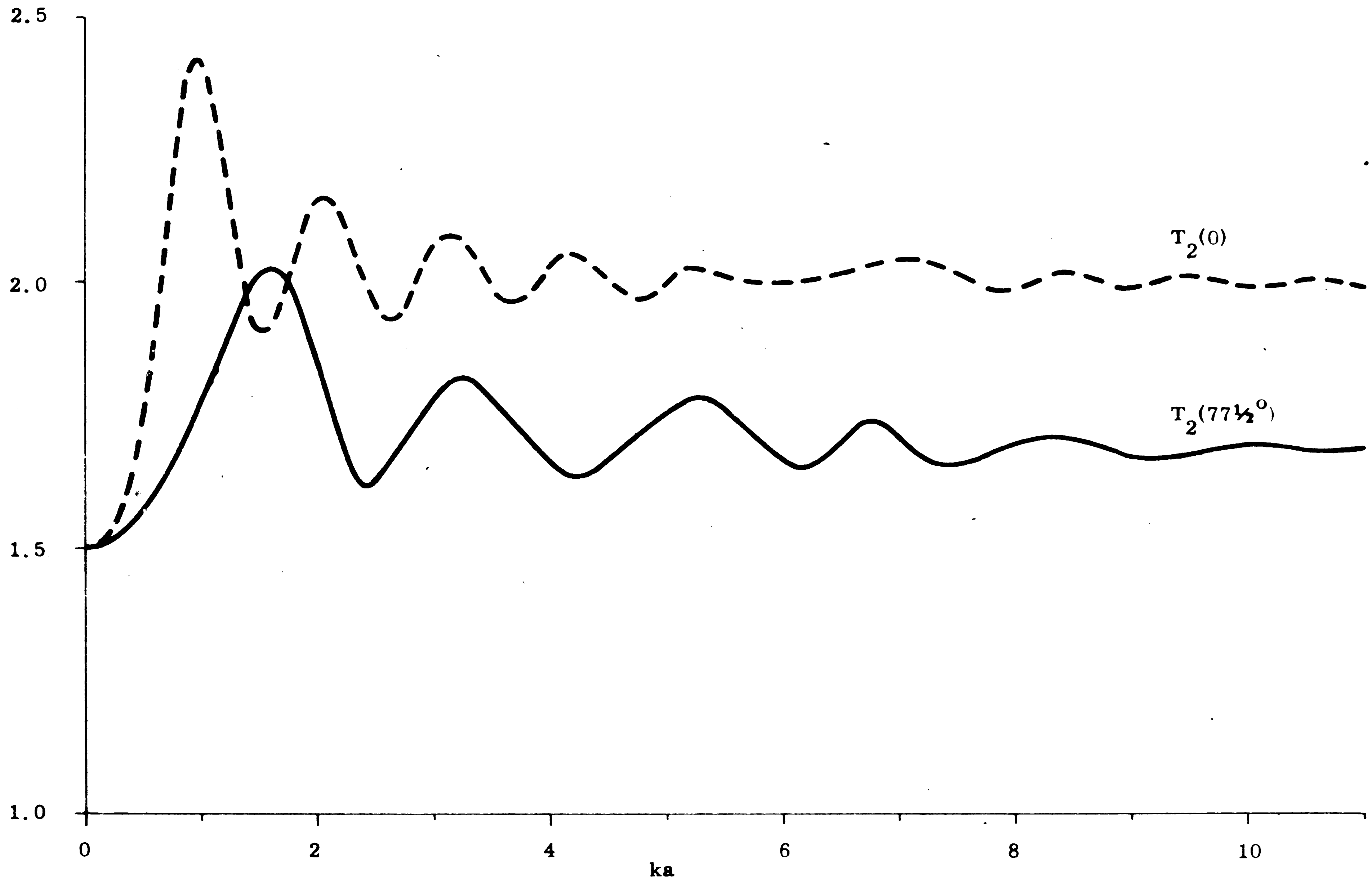

FIG. 2: $T_2(0)$ and $T_2(77\ 1/2^{\circ})$ Computed from Equation (17).

REFERENCES

1. C. J. Sletten, "Electromagnetic Scattering from Wedges and Cones," Air Force Cambridge Research Center Report No. 5090; July, 1952.

2. H. Gent, J. S. Hey and P. G. Smith, "The Echoing Area of 15° Semi-Angle Cone-Spheres with Sphere Radii between One and Two Wavelengths," presented at Symp. on the Echoing Properties of Missiles, Farnborough, England; June, 1960.

3. E. M. Kennaugh and D. L. Moffatt, "On the Axial Echo Area of the Cone-Sphere Shape," Proc. IRE, vol. 50, p. 199; February, 1962.

4. D. L. Moffatt, "Low Radar Cross Section, the Cone-Sphere," The Ohio State University Antenna Laboratory Report No. 1223-5; May, 1962.

5. J. B. Keller, "Backscattering from a Finite Cone," IRE Trans. on Antennas and Propagation, vol. AP-8, pp. 175-182; March, 1960.

6. E. M. Kennaugh and R. L. Cosgriff, "The Use of Impulse Response in Electromagnetic Scattering Problems," IRE National Convention Record, pt. 1, pp. 72-77; 1958.

7. W. E. Blore, "Experimental Measurements of the Radar Cross Section of a Cone-Sphere," Proc. IEEE, vol. 51, pp. 1263-1264; September, 1963.

8. K. M. Siegel, "Low Frequency Radar Cross Section Computations," Proc. IEEE, vol. 51, pp. 232-233; January, 1963. Note that the body here referred to as a cone-sphere is really a cone capped by a hemisphere, and the correct formula for the cross section of a cone-sphere differs from the quoted one by about 4% for small vertex angles.

9. R. E. Kleinman and T. B. A. Senior, "Diffraction and Scattering by Regular Bodies - II: The Cone," The University of Michigan Radiation Laboratory Report No. 3648-2-T; January, 1963.

10. T. B. A. Senior and R. F. Goodrich, "Scattering by a Sphere," Proc. IEE (London), vol. 111, pp. 907-916; 1964.

11. N. A. Logan, "Scattering Properties of Large Spheres," Proc. IRE, vol. 48, p. 1782; October, 1960.

12. Experimental confirmation of the fact that the larger contributor is a relatively non-directive one (i.e. a creeping wave return and not a contribution from the join) is obtainable from the back scattering pattern with vertical polarization at aspects away from nose-on.

13. N. D. Kazarinoff and T. B. A. Senior, "A Failure of Creeping Wave Theory," IRE Trans. on Antennas and Propagation, vol. AP-10, pp. 634-638; September, 1962.

14. R. F. Goodrich, B. A. Harrison, R. E. Kleinman and T. B. A. Senior, "Diffraction and Scattering by Regular Bodies - I: The Sphere," The University of Michigan Radiation Laboratory Report No. 3648-1-T; December, 1961.

15. N. A. Logan, "General Research in Diffraction Theory, Vol. II," Lockheed Missiles and Space Division Report No. LMSD-288088; December, 1959.

16. T. B. A. Senior, "Application of Surface Field Measurements to Radar Cross Section Studies," Rome Air Development Center Report No. RADC-TDR-64-25 (vol. 1, pp. 205-215); April, 1964.

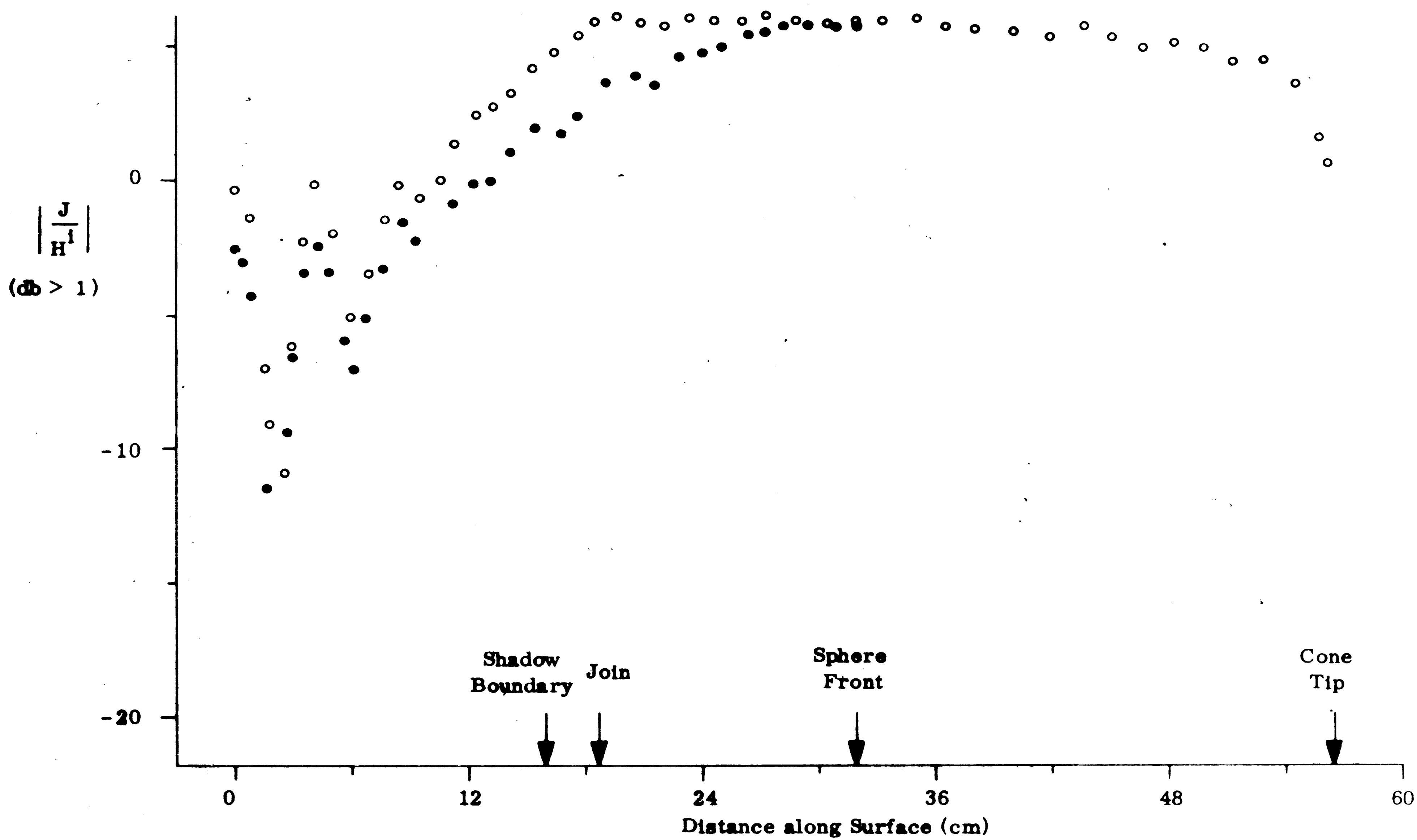

FIG. 3: Measured Current Amplitudes for a 30° Cone-Sphere (o) and Corresponding Sphere (●) at 3.714 Gc.